

ADSORPTION STUDIES ON THE REMOVAL OF Fe (II) ION FROM AQUATIC ENVIRONMENT USING NANO POROUS CARBON

R Sivakumar and S Arivoli*

*PG and Research Department of Chemistry, Thiru Vi Ka Government Arts College, Thiruvarur, Tamilnadu, India.

ABSTRACT:

The present study is on adsorption of Fe(II) ions by Activated Syringodium Isoetifolium Leaves Nano Carbon. It uses batch adsorption techniques. The influence of contact time, initial concentration, dosage of adsorbent and effect of solution pH were investigated. The equilibrium adsorption data were correlated with Langmuir, Freundlich, Temkin, Dubinin-Radushkevich, Hurkins-Jura, Halsay, Radlich-Peterson, Jovanovic and BET isotherm models. The isotherm studies of R_L values showed that the adsorption process was favorable. Thermodynamic parameters such as ΔH^0 , ΔS^0 and ΔG^0 were evaluated. The data indicate that, the adsorption was spontaneous and is an endothermic nature. Adsorption kinetics was tested with pseudo- second-order, Elovich model and intra – particle diffusion models. Kinetic studies indicate an adsorption pseudo-second-order reaction. This study shows that intra-particles played a major role in the adsorption of Fe(II) ions mechanism. The Activated Syringodium Isoetifolium Leaves Nano Carbon has high adsorption capacity and adsorption rate for the removal of Fe(II) ions from aqueous solution.

Keywords: *Adsorption, Fe(II) ions, kinetics, Activated Syringodium Isoetifolium Leaves Nano Carbon (ASI-NC), Thermodynamics,*

I INTRODUCTION

One of today's environmental challenges is the excessive use of heavy metals for industrial and domestic practices contaminates ground and surface water [1], before these pollutants discharge to the environment, it is important to remove from water and wastewater[2]. The high Fe(II) concentrations also caused gastrointestinal accumulation, low hemoglobin levels and neurotoxicity. Industries such as those involved in the production of fertilizer, petrochemicals, electroplating, tanneries, metal processing, and mining industries are released Fe(II) into the environment. [3-5]. Activated carbon has been used as a adsorbent in wastewater treatment application throughout the world ,but because of its cost in efficiency it is no longer attractive to be widely used in small-scale industries .In recent years research interest into the production of adsorbents to replace the costly activated carbon has intensified [6]. Several studies related to wastewater treatment were carried out using low-cost materials, Syringodium Isoetifolium Leaves is used as adsorbent because of it's easily available, economically viable, and biodegradable [8], and also Jordanian

Pottery materials was chosen as adsorbent due to its low cost ,its granular structure, insolubility in water, chemical stability and local availability [9].

In the present investigation the adsorption of Iron ion on activated nano carbon prepared from *Syngodium Isoetifolium Leaves Ash* by carbonization with Sulphuric acid has been achieved. The kinetic and equilibrium adsorption data obtained were utilized to characterize the sample prepared [7]. The amounts and rates of adsorption of Iron using above activated nano carbon from water were then measured. Three simplified kinetic models including pseudo first order, Pseudo second order equations and Elovich equations were used to describe the adsorption process.

II. MATERIALS AND METHODS

2.1. Adsorbent

The *Syngodium Isoetifolium* Leaves collected from East Coastal area of Nagapattinam district was Carbonized with concentrated Sulphuric Acid and washed with water and activated around 1100°C in a muffle furnace for 5 hrs the it was taken out, ground well to fine powder and stored in a vacuum desiccators.



Syngodium Isoetifolium

2.2. Chemicals

All chemicals used of high purity commercially available Analar grade. 1000 mg/L of stock solution of Iron (II) was prepared by dissolving accurately weighed 4.4786 gram of Iron (II) sulphate in 1000 ml distilled water. All experimental solutions were prepared by diluting the stock solution to the required concentration. The pH of each experimental solution was adjusted to the required initial pH value using dilute HCl (or) NaOH before mixing the adsorbent. The concentration of residual Iron (II) ion was determined with atomic absorption spectrophotometer (Perkin Elemer 2380).

2.3. Batch experiments

The effect of various parameters on the removal of Iron (II) ion onto ASI-NC was studied batch adsorption experiments were conducted at (30-60°C). For each experimental run, 50 ml of Iron (II) solution of known initial concentration and pH were taken in a 250 ml plugged conical flask. A 25 mg

adsorbent dose is added to the solution and mixture was shaken at constant agitation speed (150 rpm) sample were withdrawn at appropriate time intervals (10-60 min) and the adsorbent was separated by filtration. The residual solutions were analyzed to determine the Iron (II) ion concentration.

The effect of dosage of adsorbent on the removal of Iron (II) ion was measured by contacting 50 ml of 50 mg/L of Iron (II) ion solution with 25 mg of ASI-NC till equilibrium was attained. Adsorption equilibrium isotherm is studied using 25 mg of ASI-NC dosage per 50 ml of Iron (II) ion solution. The initial concentration were ranged from (10 to 50 mg/L) in all sets of experiments. The plugged conical flask was shaken at a speed of 150 rpm for 60 minutes. Then the solution was separated from the mixture and analyzed for Iron (II) ion concentration. The adsorption capacity was calculated by using a mass equilibrium equation as follows:

$$q_e = (C_0 - C_e) V/M \dots\dots\dots (1)$$

Where, C_0 and C_e being the initial Iron (II) concentration (mg/L) and equilibrium concentration, respectively V is the experimental volume of Iron (II) ion solution expressed in liters [L] and M is the adsorbent mass expressed in grams [g]. The Iron (II) ion ions percentage can be calculated as follows:

$$\%R = (C_0 - C_t) \times 100/C_0 \dots\dots\dots (2)$$

The effect of pH on the rate of adsorption was investigated using Iron (II) concentration of 20 mg/L constant ASI-NC dosage. The pH values were adjusted with dilute HCl and NaOH solution. The adsorbent-adsorbate mixture was shaken at room temperature using agitation speed (150 rpm) for 60 minutes. Then the concentration of Iron (II) in solution was determined.

III. RESULTS AND DISCUSSION

3.1 Effect of agitation time and initial Iron (II) ion concentration

The kinetics of adsorption of Iron (II) ion by ASI-NC is shown in Fig. 1 with smooth and single plots indicating monolayer adsorption of Iron (II) ions on the ASI-NC. The removal of Iron (II) ions increased with the lapse time and attains equilibrium in 60 min for 50 mg/ L. With increase in Iron (II) ions concentration from 10 to 50 mg/L, the amount of Iron (II) ions adsorbed increased while the percent removal decreased, indicating that the Iron (II) ions removal by adsorption on ASI-NC concentration dependent.

3.2 Effect of ASI-NC mass

The amount of Iron (II) ion adsorption increased with the increase in ASI-NC dose and reached a maximum value after a particular dose shown in Fig. 2 and taken an initial Iron (II) ions concentration of 20 mg/L, complete Iron (II) ions removal was obtained at a maximum ASI-NC dose of 125 mg. The increase in the adsorption of Iron (II) ions with ASI-NC dose was due to the introduction of more binding sites for adsorption and the availability more surface area.

3.3 Effect of pH

The experience carried out at different pH show that there was a change in the percentage removal of Iron (II) ions over the entire pH range shown in Fig. 3. This indicates the strong force of interaction between the Iron (II) ions and ASI-NC that either H^+ or OH^- ions could influence the adsorption capacity. In other words, the adsorption of Iron (II) ions on ASI-NC does involve ion exchange mechanism that have been an influence on the Iron (II) ions adsorption while varying the pH This

observation is in line with the type I and II isotherm and positive ΔH^0 value obtained, which indicates irreversible adsorption probably due to polar interactions.

3.4 Effect of other ions

The effect of other ions like Ca^{2+} and Cl^- on the adsorption process studied at different concentrations. The ions added to 50mg/L of Iron (II) ions solutions and the contents were agitated for 60 min at 30°C. The results reveals that low concentration of Cl^- does not affect the percentage of adsorption of Iron (II) ions on ASI-NC, because the interaction of Cl^- at available sites of adsorbent through competitive adsorption is not so effective. While the concentration of other ion Ca^{2+} increases, the interference of these ions at available surface sites of the sorbent through competitive adsorption increases that, decreases the percentage adsorption. The interference was more in the presence of Ca^{2+} compared with Cl^- ion. This is so because ions with smaller hydrated radii decrease the swelling pressure within the sorbent and increase the affinity of the sorbent for such ions.

3.5 Adsorption Isotherms

Adsorption isotherm describes the relation between the amount or concentration of adsorbate that accumulates on the adsorbent and the equilibrium concentration of the dissolved adsorbate. Equilibrium studies were carried out by agitating a series of beakers containing 50 mL of Iron (II) solutions of initial concentration 20 mg/L with 0.025 g of activated nano carbon at 30 °C with a constant agitation. Agitation was provided for 1.0 h, which is more than sufficient time to reach equilibrium.

3.5.1 Freundlich adsorption isotherm

The Freundlich adsorption isotherm is based on the equilibrium sorption on heterogeneous surfaces. This isotherm is derived from the assumption that the adsorption sites are distributed exponentially with respect to heat of adsorption. The adsorption isotherm is expressed by the following equation

$$q_e = K_F C_e^{1/n_F} \dots\dots\dots (3)$$

Which, can be linearized as

$$\ln q_e = \ln K_F + \frac{1}{n_F} \ln C_e \dots\dots\dots (4)$$

Where, q_e is the amount of Iron (II) adsorbed at equilibrium (mg/g) and C_e is the concentration of Iron (II) in the aqueous phase at equilibrium (ppm). K_F (L/g) and $1/n_F$ are the Freundlich constants related to adsorption capacity and sorption intensity, respectively.

The Freundlich constants K_F and $1/n_F$ were calculated from the slope and intercept of the $\ln q_e$ Vs $\ln C_e$ plot, and the model parameters are shown in Table 2. The magnitude of K_F showed that ASI-NC had a high capacity for Iron (II) adsorption from the aqueous solutions studied. The Freundlich exponent, n_F , should have values in the range of 1 and 10 (i.e., $1/n_F < 1$) to be considered as favourable adsorption [5]. A $1/n_F$ value of less than 1 indicated that Iron (II) is favorably adsorbed by ASI-NC. The Freundlich isotherm did not show a good fit to the experimental data as indicated by SSE and Chi-square statistics.

3.5.2 Langmuir adsorption isotherm

The Langmuir adsorption isotherm is based on the assumption that all sorption sites possess equal affinity to the adsorbate. The Langmuir isotherm [6] in a linear form can be represented as:

$$\frac{C_e}{q_e} = \frac{1}{q_m K_L} + \frac{C_e}{q_m} \quad \dots\dots\dots (5)$$

Where q_e is the amount of Iron (II) adsorbed at equilibrium (mg/g), C_e is the concentration of Iron (II) in the aqueous phase at equilibrium (ppm), q_m is the maximum Iron (II) uptake (mg/g), and K_L is the Langmuir constant related to adsorption capacity and the energy of adsorption (g/mg).

A linear plot of C_e/q_e Vs C_e was employed to determine the value of q_m and K_L the obtained data's were also presented in Table 2. The model predicted a maximum value that could not be reached in the experiments. The value of K_L decreased with an increase in the temperature. A high K_L value indicates a high adsorption affinity. Weber and Chakraborti expressed the Langmuir isotherm in term of dimensionless constant separation factor or equilibrium parameter (R_L) defined in the following equation:

$$R_L = \frac{1}{1 + K_L C_0} \quad \dots\dots\dots (6)$$

Where, C_0 is the initial Iron (II) concentration (ppm). Four scenarios can be distinguished:

The sorption isotherm is unfavorable when $R_L > 1$, the isotherm is linear when $R_L = 1$, the isotherm is favorable when $0 < R_L < 1$ and the isotherm is irreversible when $R_L = 0$. The values of dimensionless separation factor (R_L) for Iron (II) removal were calculated at different concentrations and temperatures. As shown in Table 3, at all concentrations and temperatures tested the values of R_L for Iron (II) adsorptions on the ASI-NC were less than 1 and greater than zero, indicating favorable adsorption.

The Langmuir isotherm showed a better fit to the adsorption data than the Freundlich isotherm. The fact that the Langmuir isotherm fits the experimental data well may be due to homogeneous distribution of active sites on the ASI-NC surface, since the Langmuir equation assumes that the adsorbent surface is energetically homogeneous.

3.5.3 Temkin adsorption isotherm:

The Temkin adsorption isotherm assumes that the heat of adsorption decreases linearly with the sorption coverage due to adsorbent-adsorbate interactions [7]. The Temkin isotherm equation is given as:

$$q_e = \frac{RT}{b_T} \ln(K_T C_e) \quad \dots\dots\dots (7)$$

Which, can be represented in the following linear form

$$q_e = \frac{RT}{b} \ln K_T + \frac{RT}{b} \ln C_e \quad \dots\dots\dots (8)$$

Where, K_T (L/g) is the Temkin isotherm constant, b_T (J/mol) is a constant related to heat of sorption, R is the ideal gas constant (8.314 J/mol K), and T is absolute temperature (K). A plot of q_e versus $\ln C_e$ enables the determination of isotherm constants K_T and b_T from the slope and intercept, the model parameters are listed in Table 2. The Temkin isotherm appears to provide a good fit to the Iron (II) adsorption data.

The adsorption energy in the Temkin model, b_T , is positive for Iron (II) adsorption from the aqueous solution, which indicates that the adsorption is endothermic. The experimental equilibrium curve is close to that predicted by Temkin model. Consequently, the adsorption isotherm of Iron (II) on ASI-NC can be described reasonably well by the Temkin isotherm.

3.5.4 Hurkins-Jura adsorption isotherm

The Hurkins-Jura [8] adsorption isotherm can be expressed as

$$q_e = \sqrt{\frac{A_H}{B_H + \log C_e}} \dots\dots\dots(9)$$

This can rearranged as follows:

$$\frac{1}{q_e^2} = \frac{B_H}{A_H} - \frac{1}{A_H} \log C_e \dots\dots\dots(10)$$

Where, A_H (g^2/L) and B_H (mg^2/L) are two parameters characterizing the sorption equilibrium.

The isotherm equation accounts for multilayer adsorption and can be explained by the existence of a heterogeneous pore distribution. The Harkins–Jura isotherm parameters are obtained from the plots of $1/q_e^2$ versus $\log C_e$ enables the determination of model parameters A_H and B_H from the slope and intercept.

3.5.5 Halsay adsorption isotherm

The Halsay [9] adsorption isotherm can be given as

$$q_e = \exp\left(\frac{\ln K_{Ha} - \ln C_e}{n_{Ha}}\right) \dots\dots\dots(11)$$

A linear form of the isotherm can be expressed as follows

$$\ln q_e = \frac{\ln K_{Ha}}{n_{Ha}} - \frac{\ln C_e}{n_{Ha}} \dots\dots\dots(12)$$

Where, K_{Ha} (mg/L) and n_{Ha} are the Halsay isotherm constants.

A plot of $\ln q_e$ Vs $\ln C_e$, enables the determination of n_{Ha} and K_{Ha} from the slope and intercept. This equation is suitable for multilayer adsorption and the fitting of the experimental data to this equation attest to the heteroporous nature of adsorbent. The experimental data and the model predictions based on the non-linear form of the Halsay models. The model parameters are listed in Table 2. This result also shows that the adsorption of Iron (II) on ASI-NC was not based on significant multilayer adsorption. The Halsay model is also not suitable to describe the adsorption of Iron (II) on ASI-NC, because this model also assumes a multilayer behavior for the adsorption of adsorbate onto adsorbent.

3.5.6 Redlich-Peterson adsorption isotherm

The Radlich-Peterson [10] adsorption isotherm contains three parameters and incorporates the features of Langmuir and Freundlich isotherms into a single equation. The general isotherm equation can be described as follows:

$$q_e = \frac{K_R C_e}{1 + a_R C_e^g} \dots\dots\dots(13)$$

The linear form of the isotherm can be expressed as follows:

$$\ln \frac{C_e}{q_e} = g \ln C_e - \ln K_R \dots\dots\dots(14)$$

Where, K_R (L/g) and a_R (L/mg) are the Radlich-Peterson isotherm constants and g is the exponent between 0 and 1. There are two limiting cases: Langmuir form for $g = 1$ and Henry's law for $g = 0$.

A plot of $\ln C_e/q_e$ versus $\ln C_e$ enables the determination of isotherm constants g and K_R from the slope and intercept. The values of K_R , presented in Table 2, indicate that the adsorption capacity of the ASI-NC decreased with an increase temperature. Furthermore, the value of g lies between 0 and 1, indicating favorable adsorption.

3.5.7 Dubinin-Radushkevich adsorption isotherm

The Dubinin-Radushkevich [11] adsorption isotherm is another isotherm equation. It is assumed that the characteristic of the sorption curve is related to the porosity of the adsorbent. The linear form of the isotherm can be expressed as follows:

$$\ln q_e = \ln Q_D - B_D \left[RT \ln \left(1 + \frac{1}{C_e} \right) \right]^2 \dots\dots\dots(15)$$

Where, Q_D is the maximum sorption capacity (mol/g), and B_D is the Dubinin-Radushkevich constant (mol^2/kJ^2). A plot of $\ln q_e$ Vs $RT \ln(1+1/C_e)$ enables the determination of isotherm constants B_D and Q_D from the slope and intercept.

3.5.8 Jovanovic adsorption isotherm

The model of an adsorption surface considered by Jovanovic¹⁶ is essentially the same as that considered by Langmuir. The Jovanovic model leads to the following relationship [12]:

$$q_e = q_{\max} \left(1 - e^{-K_J C_e} \right) \dots\dots\dots(16)$$

The linear form of the isotherm can be expressed as follows:

$$\ln q_e = \ln q_{\max} - K_J C_e \dots\dots\dots(17)$$

Where, K_J (L/g) is a parameter. q_{\max} (mg/g) is the maximum Iron (II) uptake.

The q_{\max} is obtained from a plot of $\ln q_e$ and C_e . Their related parameters are listed in Table 2. By comparing the values of the error functions, it was found the Langmuir and Temkin models are best to fit the Iron (II) adsorption on the ASI-C. Both models show a high degree of correlation. This is clearly confirming the good fit of Langmuir and Temkin models with the experimental data for removal of Iron (II) from the solution.

3.5.9 The Brunauer-Emmett-Teller (BET) isotherm model

Brunauer-Emmett-Teller (BET) isotherm is a theoretical equation, most widely applied in the gas-solid equilibrium systems [13]. It was developed to derive multilayer adsorption systems with relative concentration ranges from 10 to 50 mg/L corresponding to a monolayer coverage lying between 10 and 30 mg/L. Its extinction model related to liquid-solid interface is exhibited as:

$$q_e = \frac{q_s C_{\text{BET}} C_e}{(C_s - C_e) [1 + (C_{\text{BET}} - 1)(C_e / C_s)]} \dots\dots\dots(18)$$

Where, C_{BET} , C_s , q_s and q_e are the BET adsorption isotherm (L/mg), adsorbate monolayer saturation concentration (mg/L), theoretical isotherm saturation capacity (mg/g) and equilibrium adsorption capacity (mg/g), respectively. As C_{BET} and $C_{\text{BET}} (C_e / C_s)$ is much greater than 1,

In the linear form as used is represented as

$$\frac{C_e}{q(C_s - C_e)} = \frac{1}{q_s C_{BET}} + \left(\frac{C_{BET} - 1}{q_s C_{BET}} \right) \left(\frac{C_e}{C_s} \right) \dots\dots\dots(19)$$

Where, C_e is equilibrium Concentration (mg/l), C_s is adsorbate monolayer saturation concentration (mg/l) and C_{BET} is BET adsorption relating to the energy of surface interaction (l/mg).

3.6 Kinetic parameters

The rate and mechanism of the adsorption process can be elucidated based on kinetic studies. Iron (II) adsorption on solid surface may be explained by two distinct mechanisms: (1) An initial rapid binding of Iron (II) molecules on the adsorbent surface; (2) relatively slow intra-particle diffusion. To analyze the adsorption kinetics of the Iron (II), the pseudo-first-order, the pseudo-second-order, and intra-particle diffusion models were applied [14]. Each of these models and their linear modes of them equations presented in below.

Kinetic Models and Their Linear Forms

Model	Nonlinear Form	Linear Form	Number of Equation
Pseudo-first-order	$dq_t/dt = k_1(q_e - q_t)$	$\ln(q_e - q_t) = \ln q_e - k_1 t$	(20)
Pseudo-second-order	$dq_t/dt = k_2(q_e - q_t)^2$	$t/q_t = 1/k^2 q_e^2 + (1/q_e)t$	(21)

Where, q_e and q_t refer to the amount of Iron (II) adsorbed (mg/g) at equilibrium and at any time, t (min), respectively and k_1 (1/min), k_2 (g/mg min) are the equilibrium rate constants of pseudo-first order and pseudo-second order models, respectively.

Pseudo-first order model is a simple kinetic model, which was proposed by Lagergren during 1898 and is used for estimation of the surface adsorption reaction rate. The values of $\ln(q_e - q_t)$ were linearly correlated with t . The plot of $\ln(q_e - q_t)$ Vs t should give a linear relationship from which the values of k_1 were determined from the slope of the plot. In many cases, the first-order equation of Lagergren does not fit well with the entire range of contact time and is generally applicable over the initial stage of the adsorption processes.

In the pseudo-second order model, the slope and intercept of the t/q_t Vs t plot were used to calculate the second-order rate constant, k_2 . The values of equilibrium rate constant (k_2) are presented in Table 5. According to Table 5, the value of R^2 (0.999) related to the pseudo-second order model revealed that Iron (II) adsorption followed this model.

Nevertheless, pseudo-first order and pseudo-second order kinetic models cannot identify the mechanism of diffusion of Iron (II) into the adsorbent pores.

3.6.1 Simple Elovich Model:

The simple Elovich model [15] is expressed in the form,

$$q_t = \alpha + \beta \ln t \dots\dots\dots(22)$$

Where, q_t is the amount adsorbed at time t , α and β are the constants obtained from the experiment. A plot of q_t Vs $\ln 't'$ should give a linear relationship for the applicability of the simple Elovich kinetic. The Elovich kinetics of Iron (II) on to ASI-NC for various initial concentrations (10, 20, 30, 40 and 50 mg/L) of volume 50 mL (each), adsorbent dose 0.025g, temperature 30 °C and pH 6.5.

3.6.2 The Elovich equation

The Elovich model equation is generally expressed as

$$dq_t / dt = \alpha \exp (-\beta q_t) \dots\dots\dots(23)$$

Where; α is the initial adsorption rate ($\text{mg g}^{-1} \text{min}^{-1}$) and β is the desorption constant (g/mg) during any one experiment. To simplify the Elovich equation [16] assumed $\alpha\beta t \gg t$ and by applying boundary conditions $q_t = 0$ at $t=0$ and $q_t = q_t$ at $t = t$ Eq.(23) becomes:

$$q_t = 1/\beta \ln (\alpha\beta) + 1/\beta \ln t \dots\dots\dots (24)$$

If Iron (II) ions adsorption fits with the Elovich model, a plot of q_t vs. $\ln(t)$ should yield a linear relationship with a slope of $(1/\beta)$ and an intercept of $(1/\beta)\ln (\alpha\beta)$. The Elovich model parameters α , β , and correlation coefficient (γ) are summarized in table 5. The experimental data such as the initial adsorption rate (α) adsorption constant (β) and the correlation co-efficient (γ) calculated from this model indicates that the initial adsorption (α) increases with temperature similar to that of initial adsorption rate (h) in pseudo-second-order kinetics models. This may be due to increase the pore or active site on the ASI-NC adsorbent.

3.6.3 The Intraparticle diffusion model

The kinetic results were analyzed by the Intraparticle diffusion model [17, 20] to elucidate the diffusion mechanism. The model is expressed as:

$$q_t = K_{id} t^{1/2} + I \dots\dots\dots (25)$$

Where, 'I' is the intercept and K_{id} is the intra-particle diffusion rate constant. The intercept of the plot reflects the boundary layer effect. Larger the intercept, greater is the contribution of the surface sorption in the rate controlling step. The calculated diffusion coefficient K_{id} values are listed in Table 6. The K_{id} value was higher at the higher concentrations. Intraparticle diffusion is the sole rate-limiting step if the regression of q_t versus $t^{1/2}$ is linear and passes through the origin. In fact, the linear plots at each concentration did not pass through the origin. This deviation from the origin is due to the difference in the rate of mass transfer in the initial and final stages of the sorption. This indicated the existence of some

boundary layer effect and further showed that Intraparticle diffusion was not the only rate-limiting step.

It is clear from the Table 5 that the pseudo- second-order kinetic model showed excellent linearity with high correlation coefficient ($R^2 > 0.99$) at all the studied concentrations in comparison to the other kinetic models. In addition the calculated q_e values also agree with the experimental data in the case of pseudo-second-order kinetic model. It is also evident from Table 5 that the values of the rate constant k_2 decrease with increasing initial Iron (II) concentrations. This is due to the lower competition for the surface active sites at lower concentration but at higher concentration the competition for the surface active sites will be high and consequently lower sorption rates are obtained.

3.7. Thermodynamic treatment of the adsorption process

Thermodynamic parameters associated with the adsorption, via standard free energy change (ΔG^0), standard enthalpy change (ΔH^0), and standard entropy change (ΔS^0) were calculated as follows. The free energy of adsorption process considering the adsorption equilibrium constant K_0 is given by the equation

$$\Delta G^0 = -RT \ln K_0 \dots\dots\dots (26)$$

Where, ΔG^0 is the free energy of adsorption (kJ/mol), T is the temperature in Kelvin and R is the universal gas constant (8.314 J mol/K). The adsorption distribution coefficient K_0 for the sorption reaction was determined from the slope of the plot of $\ln(q_e/C_e)$ against C_e at different temperature. The adsorption distribution coefficient may be expressed in terms of enthalpy change (ΔH^0) and entropy change (ΔS^0) as a function of temperature,

$$\ln K_0 = (\Delta H^0/RT) + (\Delta S^0/R) \dots\dots\dots (27)$$

Where, ΔH^0 is the standard heat change of sorption (kJ/mol) and ΔS^0 is standard entropy change (kJ/mol). The value of ΔH^0 and ΔS^0 can be obtained from the slope and intercept of plot of $\ln K_0$ against $1/T$. The value of thermodynamic parameter calculated from equation 26 and 10 are shown in table 4. The thermodynamic treatment of the sorption data indicates that ΔG^0 values were negative at all temperature. The results point out that physisorption is much more favorable for the adsorption of Iron (II) ions. The positive values of ΔH^0 show the endothermic nature of adsorption and it governs the possibility of physical adsorption [18]. Because in the case of physical adsorption, while increasing the temperature of the system, the extent of Iron (II) ions adsorption increases, this rules out the possibility of chemisorptions. The low ΔH^0 value depicts Iron (II) ions is physisorbed onto adsorbent ASI-NC.

The negative ΔG^0 values table 4 were conform the spontaneous nature of adsorption Iron (II) ions onto ASI-NC. The lesser values of ΔG^0 suggest that adsorption is physical adsorption process. The positive values of ΔS^0 in table 4, showed increased randomness of the solid solution interface during the adsorption of Iron (II) ion onto ASI-NC.

In order to support that physical adsorption is the predominant mechanism, the values of activation energy (E_a) and sticking probability (S^*) were calculated from the experimental data. They were calculated using modified Arrhenius type equation related to surface coverage (θ) as follows:

$$\theta = \left(1 - \frac{C_e}{C_i}\right) \dots\dots\dots (28)$$

$$S^* = (1 - \theta)_e \frac{-E_a}{RT} \dots\dots\dots (29)$$

The sticking probability, S^* , is a function of the adsorbate/adsorbent system under consideration but must satisfy the condition $0 < S^* < 1$ and is dependent on the temperature of the system. The values of E_a and S^* can be calculated from slope and intercept of the plot of $\ln(1-\theta)$ versus $1/T$ respectively and are listed in Table 4.

From Table 4 it is clear that the reaction is spontaneous in nature as ΔG^0 values are negative at all the temperature studied. Again positive ΔH^0 value confirms that the sorption is endothermic in nature. The positive value of ΔS^0 reflects the affinities of the adsorbents for the Iron (II). The result as shown in Table 4 indicate that the probability of the Iron (II) to stick on surface of biomass is very high as $S^* \ll 1$, these values confirm that, the sorption process is physisorption.

3.8 Desorption studies

Desorption studies help to elucidate the nature of adsorption and recycling of the spent adsorbent and the Iron (II) ions. If the adsorbed Iron (II) ions can be desorbed using neutral pH water, then the attachment of the Iron (II) ions of the adsorbent is by weak bonds. The effect of various reagents used for desorption studies. The results indicate that hydrochloric acid is a better reagent for desorption, because we could get more than 90% removal of adsorbed Iron (II) ions. The reversibility of adsorbed Iron (II) ions in mineral acid or base is in agreement with the pH dependent results obtained. The desorption of Iron (II) ions by mineral acids and alkaline medium indicates that the Iron (II) ions was adsorbed onto the ASI-NC through physisorption as well as by chemisorptions mechanisms [19].

IV CONCLUSION

The adsorption of Fe(II) on to Activated Syringodium Isoetifolium Leaves Nano Carbon was investigated in this research work. The adsorption equilibrium well correlated with both Langmuir and BET isotherm models. The adsorption kinetic process was found pseudo-second-order model. Isotherm and kinetic study indicates that the ASI-NC can be effectively employed for the adsorption of Fe(II) ions. Thermodynamic results show that adsorption of Fe(II) ions on to ASI-NC was spontaneous and physical adsorption.

REFERENCES

1. Amin, N.K. Removal of reactive dye from aqueous solutions by adsorption onto activated carbons prepared from sugarcane bagasse pith. *Desalination*, 223(1) (2008) 152-161.

2. Amin, N.K. Removal of direct blue-106 dye from aqueous solution using new activated carbons developed from pomegranate peel: Adsorption equilibrium and kinetics. *Journal of hazardous materials*, 165(1-3) (2009) 52-62.
3. Gad, H.M. and A.A. El-Sayed. Activated carbon from agricultural by-products for the removal of Rhodamine-B from aqueous solution. *Journal of Hazardous Materials*, 168(2) (2009) 1070-1081.
4. Ganesh, P.S., E. Ramasamy, S. Gajalakshmi and S. Abbasi. Extraction of volatile fatty acids (VFAs) from water hyacinth using inexpensive contraptions and the use of the VFAs as feed supplement in conventional biogas digesters with concomitant final disposal of water hyacinth as vermicompost. *Biochemical engineering journal*, 27(1) (2005) 17-23.
5. Rahman, M.A. S.R. Amin and A.S. Alam. Removal of Methylene Blue from Waste Water Using Activated Carbon Prepared from Rice Husk. *Dhaka University Journal of Science*, 60(2) (2012)185-189.
6. Arivoli S, V Marimuthu and ARM Jahangir. Equilibrium, kinetic and thermodynamic study on copper (ii) removal from aqueous solution using *Strychnos nux-vomica* L. *International Journal of Bioassays*, 4(01) (2015) 3611-3617.
7. Arivoli, S. T, Rose Judith and V Marimuthu. Kinetic, Equilibrium and Mechanistic Studies of Nickel Adsorption on Activated Pistia Stratiotes Leaves, *European Journal of Applied Sciences and Technology [EUJAST]*, 1(1) (2014) 15-22.
8. Arivoli, S. T, Rose Judith and V Marimuthu. Kinetic, Equilibrium and Thermodynamics Studies on the Removal of Iron (III) Onto Activated Pistia Stratiotes Leaves Nano Carbon, *Research and Reviews: Journal of Chemistry*, 3(1) (2014) 15-22.
9. Ho Y S , McKay G, "The kinetic of sorption of divalent metal ions on to Sphagnum moss peat" *Water Res.* 34 (2000) 735 – 742.
10. Spark D L, "Kinetics of Reaction in pure and mixed system in soil physical chemistry", CRC, Press, Boca Raton. (1986).
11. Weber T W, Chakravorti R K, "Pore and Solid diffusion models for fixed bed adsorbers". *J. Am. Inst, Chem. Eng*, 20 (1974) 228.
12. Hammed BH, "A novel agricultural waste adsorbent for the removal of cationic dye from aqueous solution" *Journal of hazardous materials.*,162 (2009) 305- 311.

13. Freundlich H, "The dye adsorption is losungen (Adsorption in Solution)", Z Phys, Chem. 57 (1906) 385 – 470.
14. Langmuir I, "The adsorption of gases plane surfaces of glass, mica and platinum". J. Am.Soc., 579 (1918) 1361 – 1403.
15. Gupta, G. S. Prasad, G. Singh, V. N. "Removal of Chrome Dye from Carpet Effluents using Coal II (Rate process)". Environ. Technol. Lett. 9 (1988) 1413.
16. Khan, A A, Singh, R P. Adsorption thermodynamics of carbofuran on Sn (IV) arsenosilicate in H^+ , Na^+ and Ca^{2+} forms, Colloid & Surfaces (24) (1987) 33 – 42
17. Allen, S. J. Mckay, G. Khader, K. Y. H. "Intraparticle Diffusions of Basic Dye during Adsorption onto Sphagnum Peat". Environ. Pollut. 56 (1989) 39.
18. Al Duri, B. Mckay, G. El Geundi, M. S. Wahab Abdul, M. Z. "Three Resistance Transport Model for dye Adsorption onto Bagasse Pitch". J. Environ. Eng. Div. ASCE, 116 (1990) 487.
19. Chien S H, Clayton W R, "Application of Elovich Equation to the kinetics of Phosphate release and sorption on soil", Soil Sci. Soc, Am. J. 44 (1980) 265 – 268.
20. Weber W J, Morris J C, "Kinetics of adsorption on Carbon from solution". J, Sanitary Eng, Div. 90 (1964) 79.

TABLE: 2. EQUILIBRIUM PARAMETERS FOR THE ADSORPTION OF Fe(II) ION ONTO ASI-NC

M_0	C_e (Mg / L)				Q_e (Mg / L)				Removal %			
	30°C	40°C	50°C	60°C	30°C	40°C	50°C	60°C	30°C	40°C	50°C	60°C
10	2.216	1.716	1.466	1.441	15.57	16.57	17.07	17.12	77.84	82.84	85.34	85.59
20	3.716	3.467	3.226	2.716	32.57	33.07	33.55	34.57	81.42	82.67	83.87	86.42
30	6.986	6.417	5.716	5.367	46.03	47.17	48.57	49.27	76.71	78.61	80.95	82.11
40	9.737	8.987	8.574	8.103	60.53	62.03	62.85	63.79	75.66	77.53	78.56	79.74
50	13.97	13.51	13.24	12.51	72.07	72.97	73.52	74.98	72.07	72.97	73.52	74.98

TABLE: 3. ISOTHERMS PARAMETER FOR THE ADSORPTION OF Fe(II) ION ONTO ASI-NC

Model	Constant	Temperature (° C)			
		30	40	50	60
Freundlich	K_f (mg/g) (L/mg) ^{1/n}	9.495	12.212	14.224	15.274
	n	1.2477	1.3918	1.4878	1.4961

Langmuir	Q_m (mg/g)	183.77	140.57	124.98	125.64
	K_L (L/mg)	0.0483	0.0823	0.1116	0.1222
Temkin	b_T (J/mol)	30.008	27.474	26.139	26.619
	K_T (L/mg)	0.9042	0.9997	1.0513	1.0711
Hurkins-Jura	A_H (g^2/L)	-226.68	-272.50	-304.77	-318.05
	B_H (mg^2/L)	-1.0510	-1.0305	-1.0134	-0.9891
Halsay	K_{Ha} (mg/L)	16.582	32.553	51.933	59.062
	n_{Ha}	1.2477	1.3918	1.4878	1.4961
Radlich-Peterson	g	0.1985	0.2815	0.3279	0.3316
	K_R (L/g)	0.1053	0.0819	0.0703	0.0655
Dubinin-Radushkevich	q_s (mg/g)	64.799	61.921	61.636	65.179
	$K_D \times 10^{-4}$ mol ² kJ ⁻²	1.4987	1.4830	1.4780	1.4876
Jovanovic	K_J (L/g)	0.1169	0.1155	0.1131	0.1178
	q_{max} (mg/g)	16.970	18.684	20.202	20.914
BET	C_{BET} (L/mg)	4.3033	4.5052	6.1156	7.3146
	q_s (mg/g)	0.2324	0.2220	0.1635	0.1367

TABLE: 4. DIMENSIONLESS SEPERATION FACTOR (R_L) FOR THE ADSORPTION OF Fe(II) ION ONTO ASI-NC

(C_i)	Temperature °C			
	30°C	40°C	50°C	60°C
10	0.4531	0.3269	0.2638	0.2466
20	0.2929	0.1954	0.1520	0.1406
30	0.2164	0.1394	0.1067	0.0984
40	0.1716	0.1083	0.0822	0.0756
50	0.1422	0.0885	0.0669	0.0614

TABLE: 5. THERMODYNAMIC PARAMETER FOR THE ADSORPTION OF Fe(II) ION ONTO ASI-NC

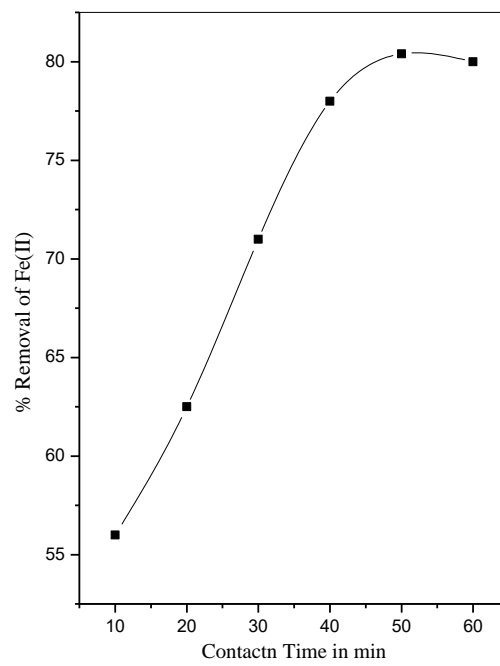
(C_0)	ΔG°				ΔH°	ΔS°	Ea	S^*
	30°C	40°C	50°C	60°C				
10	-3165.3	-4097.2	-4729.6	-4932.9	14.934	60.268	12266.9	0.0016
20	-3722.3	-4065.0	-4426.9	-5123.1	10.040	45.203	8428.94	0.0067
30	-3003.1	-3387.1	-3884.7	-4218.9	9.5753	41.506	7614.04	0.0114
40	-2856.8	-3223.3	-3488.0	-3793.8	6.4659	30.838	5027.34	0.0329
50	-2387.8	-2584.4	-2742.8	-3038.9	3.9880	20.995	2931.67	0.0876

TABLE: 6. THE KINETIC PARAMETERS FOR THE ADSORPTION OF Fe(II) ION ONTO ASI-NC

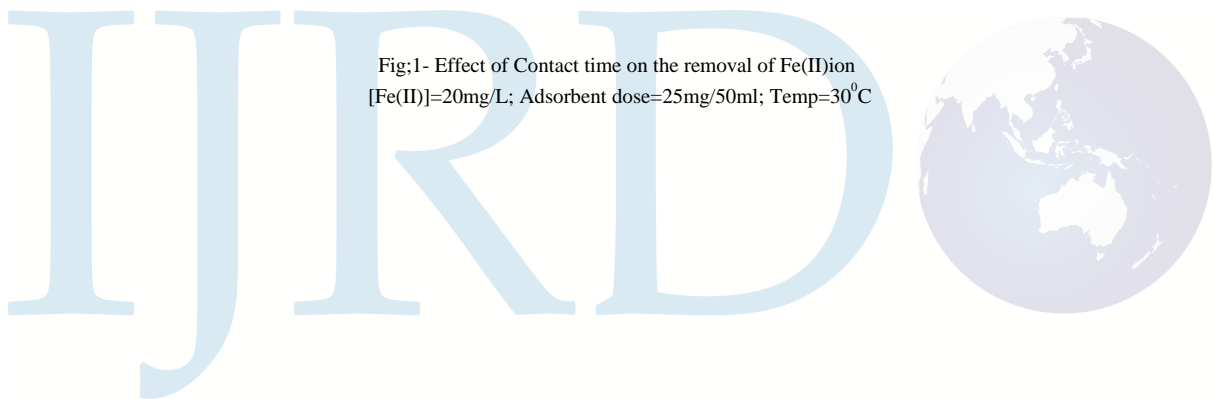
C_0	Temp °C	Pseudo second order				Elovich model			Intraparticle diffusion		
		q_e	k_2	γ	h	α	β	γ	K_{id}	γ	C
10	30	15.78	0.0160	0.9901	3.985	0.00	0.5615	0.9939	0.0175	0.9889	1.880
	40	17.88	0.0097	0.9902	3.096	85.09	0.4787	0.9866	0.1399	0.9881	1.663
	50	17.85	0.0165	0.9959	5.247	4224	0.7172	0.9868	0.0872	0.9909	1.772
	60	17.85	0.0176	0.9929	5.596	8046	0.7557	0.9879	0.0822	0.9920	1.782

20	30	35.95	0.0034	0.9963	4.426	45.91	0.2003	0.9922	0.1754	0.9942	1.585
	40	36.19	0.0038	0.9909	5.002	68.12	0.2097	0.9877	0.1633	0.9909	1.616
	50	36.55	0.0044	0.9943	5.817	109.3	0.2200	0.9872	0.1511	0.9935	1.649
	60	37.04	0.0049	0.9904	6.734	256.1	0.2427	0.9889	0.1319	0.9952	1.694
30	30	49.05	0.0037	0.9912	8.928	625.9	0.1997	0.9926	0.1196	0.9892	1.659
	40	50.78	0.0040	0.9970	10.44	513.4	0.1837	0.9867	0.1254	0.9883	1.672
	50	52.81	0.0034	0.9955	9.547	220.0	0.1576	0.9890	0.1439	0.9875	1.652
	60	52.41	0.0050	0.9971	13.66	901.5	0.1856	0.9868	0.1184	0.9877	1.708
40	30	64.99	0.0037	0.9945	15.53	520.0	0.1362	0.9906	0.1321	0.9896	1.651
	40	66.48	0.0035	0.9904	15.26	525.8	0.1336	0.9883	0.1320	0.9905	1.659
	50	67.13	0.0037	0.9934	16.63	721.4	0.1369	0.9930	0.1266	0.9926	1.675
	60	68.09	0.0037	0.9965	17.12	825.5	0.1370	0.9886	0.1243	0.9937	1.686
50	30	77.01	0.0022	0.9912	12.82	473.4	0.1162	0.9888	0.1330	0.9924	1.607
	40	78.06	0.0021	0.9972	12.94	471.3	0.1145	0.9881	0.1333	0.9945	1.612
	50	78.23	0.0023	0.9906	13.97	772.3	0.1212	0.9888	0.1241	0.9892	1.632
	60	79.97	0.0021	0.9930	13.39	537.5	0.1133	0.9917	0.1311	0.9892	1.627





Fig;1- Effect of Contact time on the removal of Fe(II)ion
[Fe(II)]=20mg/L; Adsorbent dose=25mg/50ml; Temp=30°C



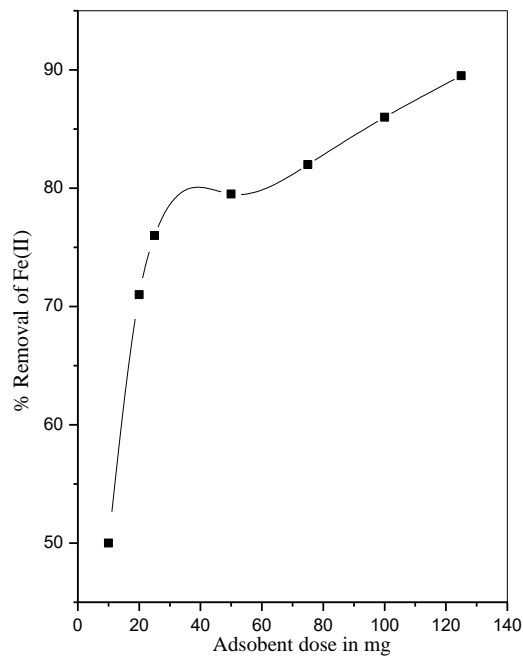


Fig:2- Effect of Adsorbent dose on the removal of Fe(II)ion
[Fe(II)]=20mg/L; Contact time=50min; Dose=25mg/50ml;Temp=30°C

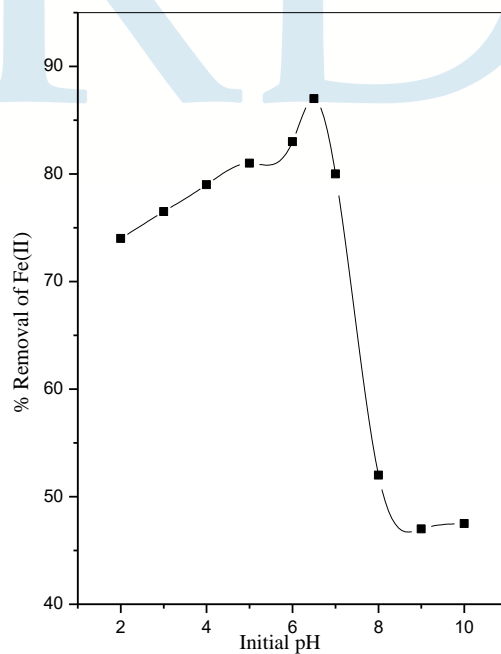


Fig:3- Effect of Initial pH on the removal of Fe(II)ion
[Fe(II)]=20mg/L; Contact time=50min; Dose=25mg/50ml;Temp=30°C